A Theoretical Model for Predicting Adiabatic Short Tube

J. M. Yin

ACRC TR-136 February 1998

For additional information:

Air Conditioning and Refrigeration Center
University of Illinois
Mechanical & Industrial Engineering Dept.
1206 West Green Street
Urbana, IL 61801

(217) 333-3115

Prepared as part of ACRC Projects 69 and 78
Stationary Air Conditioning System Analysis
W. E. Dunn and C. W. Bullard, Principal Investigators
and
Modeling, Diagnostics, and Control for Mobile Air-Conditioning Systems
W. E. Dunn and N. R. Miller, Principal Investigators

The Air Conditioning and Refrigeration Center was founded in 1988 with a grant from the estate of Richard W. Kritzer, the founder of Peerless of America Inc. A State of Illinois Technology Challenge Grant helped build the laboratory facilities. The ACRC receives continuing support from the Richard W. Kritzer Endowment and the National Science Foundation. The following organizations have also become sponsors of the Center.

Amana Refrigeration, Inc.
Brazeway, Inc.
Carrier Corporation
Caterpillar, Inc.
Copeland Corporation
Dayton Thermal Products
Delphi Harrison Thermal Systems
Eaton Corporation
Ford Motor Company
Frigidaire Company
General Electric Company
Hydro Aluminum Adrian, Inc.
Indiana Tube Corporation
Lennox International, Inc.
Modine Manufacturing Co.
Peerless of America, Inc.
Redwood Microsystems, Inc.
The Trane Company
Whirlpool Corporation
York International, Inc.

For additional information:

Air Conditioning & Refrigeration Center
Mechanical & Industrial Engineering Dept.
University of Illinois
1206 West Green Street
Urbana IL 61801

217 333 3115

TABLE OF CONTENTS

A Theoretical Model for Predicting Adiabatic Short Tube Performance for R134a

ABSTRACT

A new theoretical model for predicting short tube orifice performance is presented. The new model can be used over wide parameter ranges, with subcooling from 0°C to 50 °C, inlet pressures as high as 35bar, and inlet quality from 0 to 0.98.

The comparison of the model predictions to the nearly thousand experimental data for quality and subcooled inlet conditions, for tubes with and without screens and for different diameters and length, provided a comprehensive assessment of the model's accuracy. The model can predict the mass flow rate of with screen tubes within ±10% by using nominal diameter, if the measured diameters were used, the deviations can be reduced further.

For quality inlet and low subcooling inlet data, the present model is essentially the same as that for capillary tube case with metastable correction. For data with high subcooling, a new model is proposed based on the thermodynamic analysis that the flow can not be choked within the tube, but the experimental results shown that the flow is choked. The only way for refrigerant flow through the tube is choked just outside of the tube exit plane, and the choked pressure is the vaporization pressure, which is calculated from the corresponding saturation pressure and metastable correction.

INTRODUCTION

The short (orifice) tube is a constant area expansion device, has no moving parts, nothing to wear out, and is simple and inexpensive. It is widely used in residential air-conditioners, heat pumps and mobile air-conditioning systems as the expansion device. The primary purpose of a short tube orifice was to control refrigerant flow in the system by the throttling of refrigerant from the high pressure side (condenser) to the low pressure side (evaporator).

Most previous on flow work through orifices has focused on water. Pasqua [1] studied the flow of subcooled and saturated liquid R12 through short tube with $4<L/D<24$. For subcooled liquid entering the short tube, it was observed from his visual study that a metastable inner core of liquid was surrounded by a two-phase annular ring inside the short tube. He concluded that a metastable liquid core increased the flow rate compared to when the flow flashed inside the tube. The existence of a metastable flow in the short tube was confirmed by other researchers [2-4].

Constant flow area expansion devices, such as capillary and short tubes, should choke the flow of refrigerant to maintain proper system operation and reliability. In other words, the flow rate should be insensitive to downstream pressure. Aaron and Domanski [5] recommended that the L/D ratio should be larger than 5 to ensure choked flow under a wide range of operating conditions.

Most of the short tube flow models have been developed by empirically correcting the orifice constant, C, and downstream pressure in the general orifice equation [1, 5-7]. Several researchers have developed two-phase critical flow models for water [8, 9]. However there are no published theoretical models that can predict the mass flow rate of short tube in the quality inlet case and subcooled inlet case for refrigerant.

The purposes of this work are to study the applicability of the capillary tube model to short tube, and to develop a new model for subcooled inlet data with high subcooling.

GOVERNING EQUATIONS

The fundamental equations governing the short tube flow include the continuity, conservation of momentum, and conservation of energy equations. In modeling the flow, these governing equations along with the second law of thermodynamics must be satisfied through both the single phase subcooled liquid region and the two-phase liquid/vapor region. Initially, the following additional assumptions are proposed:

- adiabatic flow with no externally applied work
- thermodynamic equilibrium through the two-phase region
- homogeneous two-phase flow

The homogeneous flow assumption was based on the results of several previous capillary tube research efforts. These included the modeling work by Bittle et al. [10] and Kuehl et al. [11].

Continuity Equation

An axial differential length dx is shown in Figure 1. Applying the continuity equation at the inlet and exit plane of the incremental length

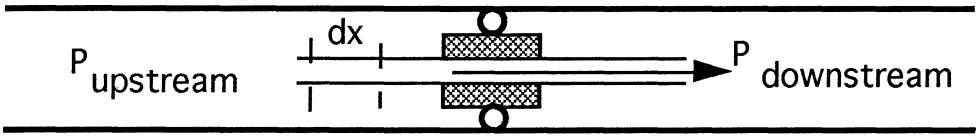

Figure 1 Flow model incremental length

results in the mass flow rate $\dot{m}$

$$\dot{m} = V_1 A_1 / v_1 = V_2 A_2 / v_2 \qquad (1)$$

Here V, A, and v represent the fluid velocity, cross-sectional area of the tube and the specific volume of the fluid; subscripts 1 and 2 denote the inlet and exit planes of the incremental section. For the tube, the cross-sectional area is assumed to be constant throughout the length of the tube, and equation 1 reduces to

$$V_1 / v_1 = V_2 / v_2 \qquad (2)$$

In the case of the subcooled liquid region that may exist in the upstream portion of the tube, the adiabatic assumption translates to a constant fluid temperature that is equal to the inlet temperature. The specific volume can also be assumed to be constant, and Equation 2 reduces to

$$V_1 = V_2 \tag{3}$$

which states that the velocity is constant through the subcooled liquid region.

Downstream of the point of the onset of vaporization, i.e., the flash point, the refrigerant quality increases as the pressure decreases. Therefore, the assumption of a constant specific volume does not apply, and Equation 2 is the appropriate form of the continuity equation.

The mass flux G is defined as

$$G = \dot{m}/A \tag{4}$$

Momentum Equation

The momentum equation can be expressed as

$$\frac{-dp}{dx} = \frac{fvG^2}{2D_c} + G^2\frac{dv}{dx} \tag{5}$$

where Dc is the diameter of the capillary tube, and f is the friction factor. The left side of Equation 5 shows the pressure drop dp across the differential length dx; the right side of Equation 5 shows that this pressure drop is caused by friction and fluid acceleration.

Through the subcooled liquid region, because the liquid is incompressible (dv=0 in Equation 5), the total pressure drop is due only to friction. For subcooled liquid region, Equation 5 reduces to

$$-dp = \frac{fvG^2}{2Dc}dx \tag{6}$$

Equation 6 can be used to calculate dp or dx if the other is known.

Through the two-phase region, however, the acceleration component can be significant since the specific volume is increasing as the quality increases. The appropriate form of Equation 5 through the two phase region is

$$-\Delta P = (P_1 - P_2) = \frac{f_m v_m G}{2D_c}\Delta L + G^2\Delta v \tag{7}$$

where f_m, v_m are average values across the incremental length ΔL given by

$$f_m = \frac{f_1 + f_2}{2} \tag{8}$$

$$v_m = \frac{v_1 + v_2}{2} \tag{9}$$

Energy Equation

The energy conservation equation can be expressed as

$$\frac{dh}{dx} = \frac{-G^2}{2}\frac{d(v^2)}{dx} \tag{10}$$

Applying this equation to a segment with length of ΔL, it can be rewritten as

$$h_1 - h_2 = \frac{-G^2}{2}(v_1^2 - v_2^2) \tag{11}$$

In the subcooled liquid region, $v_1^2 = v_2^2$ (incompressible), so Equation 11 reduces to

$$h_1 = h_2 \tag{12}$$

Since the change in enthalpy for a subcooled liquid can be considered to be a function of temperature only, Equation 12 implies that through the subcooled liquid region there is no change in the refrigerant temperature.

In the two-phase region, the enthalpy and specific volume are calculated using

$$h = h_f + x(h_g - h_f) \tag{13}$$

$$v = v_f + x(v_g - v_f) \tag{14}$$

Equation 11 together with Equations 13 and 14 can be used to calculate the exit quality of the segment by knowing the inlet quality and specific volume of the segment.

FRICTION FACTOR AND VISCOSITY FOR TWO-PHASE FLOW

To solve the above governing equations, friction factors for both subcooled liquid and two-phase fluid must be determined. There are many correlations published for the single phase friction factor. The correlation used in this study is an explicit curve fit that approximates the transcendental Colebrook friction factor for smooth-tube single phase turbulent flow [12]

$$f = 0.25[\log(\frac{e/D_c}{3.7} + \frac{5.74}{Re^{0.9}})]^{-2} \tag{15}$$

where e is the roughness of the capillary tube and Re is the Reynolds number, which is defined as

$$Re = \frac{\rho V D_c}{\mu} = \frac{G D_c}{\mu} \tag{16}$$

where ρ is the density and μ is the viscosity of the refrigerant.

Equation 15 was developed for calculating the friction factor for single phase flow, using liquid or vapor viscosity in Equation 16. In order to calculate the friction factor of the refrigerant in the two-phase region, the commonly used method is take the same function as Equation 15 and

using some proper mixing rules to calculate the two-phase viscosity μ in Reynolds number from the corresponding saturated liquid viscosity μ_f and saturated vapor viscosity μ_g.

Two-phase viscosity models that are reported in the literature include

(i) the McAdams model [13], given by

$$\frac{1}{\mu} = \frac{1-x}{\mu_f} + \frac{x}{\mu_g} \tag{17}$$

(ii) the Cicchitti model [14], given by

$$\mu = x\mu_g + (1-x)\mu_f \tag{18}$$

(iii) the Dukler model [15], given by

$$\mu = \frac{[xv_g\mu_g + (1-x)v_f\mu_f]}{v} \tag{19}$$

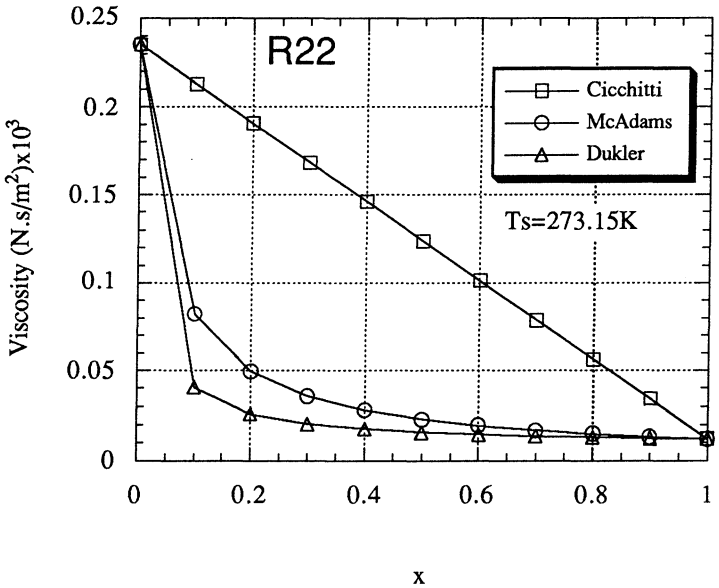

Figure 2 Viscosity changes along quality from different models for R22

Figure 2 shows the difference of the three viscosity models. It is clear that at the same saturation temperature and quality, Cicchitti model gives the highest viscosity, and the Dukler model the lowest, from the definition of Reynolds number, it follows that the Cicchitti model corresponds to the lowest Reynolds number and highest friction factor, while the Dukler model gives the lowest friction factor due to its higher Reynolds number.

Among the three mixings, Cicchitti's mixing rule is simply a liner interpolation of the saturated liquid and vapor viscosity on quality; McAdams and Dukler mixing rule have large difference in low quality region. Because the Dukler's mixing rule is derived based on reasonable physical models, it is selected in the present study.

ENTRANCE LOSS CORRECTION FACTOR

The entrance to the orifice tube can be characterized as a sudden contraction from a large diameter tube to the orifice tube diameter. Collier and Thomas [16] reported a correlation to calculate the pressure drop associated with a sudden contraction. It is given by

$$\Delta P_{entrance} = \frac{G^2}{2\rho}[(\frac{1}{C_c}-1)^2 + (1-\frac{1}{\theta^2})][1+\frac{v_g}{v_f}x]$$

$$= \frac{G^2 v}{2}(1+K)[1+\frac{v_g}{v_f}x] \qquad (20)$$

where θ is the ratio of the flow areas before and after the contraction, v is the specific volume, ρ is the density and C_c is given by

$$C_c = \frac{0.554}{\theta^3} - \frac{0.242}{\theta^2} + \frac{0.111}{\theta} + 0.585 \qquad (21)$$

As can be seen in Equation 20, the kinetic energy term $G^2v/2$ is modified empirically to include the effects of the relative cross-sectional areas θ, the vapor-to-liquid specific volume ratio, and the inlet quality, x. For a subcooled inlet condition, the quality x in Equation 20 is zero.

Idelchik [17] pointed out that the pressure drop due to acceleration plus entrance loss for turbulent single phase flow($Re>10^4$) can be calculated from

$$\Delta P_{entrance} = (1+K)\frac{vG^2}{2} \qquad (22)$$

where K=0.5 for sudden contraction from a large tube to a small tube. As shown in Table 1, when the areas ratio θ is larger than 10 (this is practically true as shown in Figure 1), so the entrance loss coefficient K from Equation 20 is very close to 0.5.

Table 1 K values calculated from Equation 20

q	1	1.5	3	5	10	15	20	25
1+K	0	0.718	1.2788	1.3976	1.4563	1.4526	1.4804	1.4850

For the experimental reported in this paper, θ ranged from 33.3 to 66.7.

CRITICAL FLOW

A critical or choked flow condition can exist at the short tube exit plane when the evaporation pressure is lower than the critical exit pressure. The critical exit pressure is the exit plane pressure corresponding to the critical flow condition. Lowering the evaporator pressure below the critical pressure will not result in an increase in the mass flow rate through the tube.

A critical flow or choked flow means that the velocity of the fluid at the exit plane reaches the sonic velocity, c, defined as

$$c = \sqrt{(\partial P / \partial \rho)_{s=const}} = v\sqrt{-(\partial P / \partial v)_s} \tag{23}$$

in the single phase region, assuming that the fluid flow in the capillary tube near the exit plane is isentropic.

For practical calculation the critical mass flux G_c is more useful than the sound velocity. It can be calculated from the following equation if the exit plane flow process is a isentropic one

$$G_c = \rho\sqrt{(\partial P / \partial \rho)_s} = \sqrt{-(\partial P / \partial v)_s} \tag{24}$$

Practically, because of the refrigerant in the exit section of the capillary tube is a two-phase mixture, how to calculate the sound velocity (or critical mass flux) of refrigerant in two-phase region is still a problem.

Hsu and Graham [19] present the following general equation for two-phase flow critical mass flux:

$$G_c^2 = -\frac{1}{\frac{\partial}{\partial P}\{\frac{[\Psi(1-x)v_f + xv_g][x\Psi + (1-x)]}{\Psi}\}} \tag{25}$$

where, Ψ is the slip ratio, v_f and v_g are the specific volume at saturated liquid and saturated vapor state, x is the quality. It is a useful equation for classifying the different two-phase critical mass flux calculation models.

The critical mass flux (or sound velocity) of the two-phase refrigerant at the exit plane of the capillary tube depends on the model chosen. Generally, the models can be divided into three broad categories: homogeneous equilibrium models (HEM); homogeneous frozen models (HFM); and nonhomogeneous models. The homogeneous equilibrium models may assume that the fluid flows isentropically at the exit plane (called HESM), or isenthalpically (HEHM).

The homogeneous equilibrium models assume that the vapor and liquid velocities are equal so that the slip ratio is unity,

$$\Psi = \frac{V_g}{V_f} = 1 \tag{26}$$

resulting in

$$G_c = -\frac{\partial P}{\partial v} \tag{27}$$

The Homogeneous Equilibrium Isentropic Model (HESM) is derived based on the assumption that the flow process of the exit plane is isentropic

$$v = v_f + x(v_g - v_f)$$

$$\frac{dv}{dP} = \frac{dv_f}{dP} + \frac{d[x(v_g - v_f)]}{dP} = \frac{dv_f}{dP} + (v_g - v_f)\frac{dx}{dP} + x\frac{d(v_g - v_f)}{dP}$$

$$x = \frac{s - s_f}{s_g - s_f}$$

$$\frac{dx}{dP} = -\frac{ds_f}{dP(s_g - s_f)} - \frac{x}{(s_g - s_f)}\frac{d(s_g - s_f)}{dP}$$

Putting these Equations into Equation 27, the following equation for critical mass flux can be derived for HESM

$$G_c = \{\frac{-1}{\frac{dv_f}{dP} - (\frac{v_{fg}}{s_{fg}})\frac{ds_f}{dP} + x[\frac{dv_{fg}}{dP} - (\frac{v_{fg}}{s_{fg}})\frac{ds_{fg}}{dP}]}\} \quad (28)$$

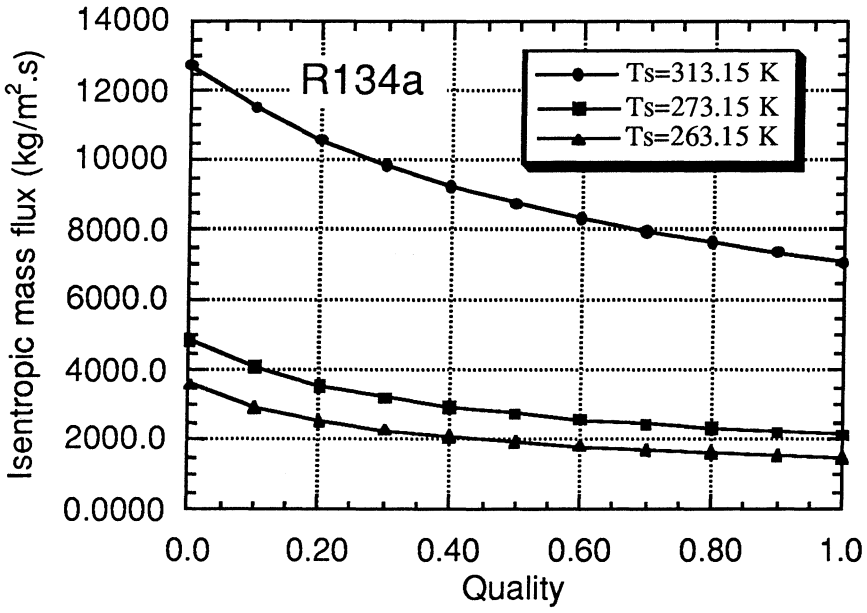

Figure 3 Isentropic mass flux for R134a for different qualities at different saturation temperature

Figure 3 shows the results for R134a calculated from homogeneous equilibrium isentropic model.

Using the similar method, suppose enthalpy at the exit plane is a constant, the following equation for isenthalpic flow (HEHM) can be derived

$$G_c = \{\frac{-1}{\frac{dv_f}{dP} - (\frac{v_{fg}}{h_{fg}})\frac{dh_f}{dP} + x[\frac{dv_{fg}}{dP} - (\frac{v_{fg}}{h_{fg}})\frac{dh_{fg}}{dP}]}\} \quad (29)$$

The homogeneous frozen model (HFM) is derived from Equation 25 based on the assumption that the quality near the exit plane of the tube is a constant so the derivative of quality with respect to pressure is zero. There are three different HFM methods presented in the literature include Smith [20], Wallis [21]. As pointed out by Pate and Tree [22], the three HFM methods follow a similar pattern, even though the equations are quite dissimilar. Following Pate and Tree, the HESM model was selected for this analysis.

METASTABLE CORRECTION

For the case of the subcooled inlet condition, the thermodynamic equilibrium flash point theoretically occurs at the point at which the refrigerant pressure is equal to the saturation pressure corresponding to the refrigerant temperature. In actuality, the flash point does not occur at this point, due to the fact that a finite amount of superheat is required for the formation of the first vapor bubble. The net result is that the a liquid region exists at pressures below saturation pressure where thermodynamic equilibrium should not allow a liquid to exist. The effect of the metastable liquid region is that the actual orifice tube flow rate will be greater than the flow rate that would exist under ideal thermodynamic equilibrium conditions. This phenomena was observed experimentally by many researchers.

A metastable flow model presented by Chen [23] predicts under pressure associated with the delay of vaporization, based on experiments with R12:

$$\frac{(P_s - P_v)(kT_s)^{0.5}}{\sigma^{1.5}}$$

$$= 0.679(\frac{v_g}{v_g - v_f})Re^{0.914}(\frac{\Delta T_{sc}}{T_c})^{-0.208}(\frac{d_c}{D'})^{-3.18} \quad (30)$$

In Equation 30, Tc is the critical temperature, Ts is the liquid temperature, k is the Boltzmann's constant ($k=1.380662x10^{-23}$J/molecule.K. Theoretically, kT is the molecular collision force), σ is the liquid refrigerant surface tension, dc is the diameter of the capillary tube, and D' is the reference length given by

$$D' = (\frac{kTs}{\sigma})^{0.5}x10^4 \quad (31)$$

Under pressure Ps-Pv=ΔPsv is defined as the difference between the saturation pressure corresponding to the liquid temperature and the actual pressure associated with the onset of vaporization.

The empirical constants in Equation 31 were determined based on the experimental data with R12 in a limited parameter range.

Several studies introduced the Chen's metastable correction in their capillary tube models, Dirik [24] used this correction for R134a within the specified parameter ranges with apparent success, but Bittle and Pate [10] found that it is not suitable for R22.

For short tube, if the inlet is in subcooled region, the flow phenomena may be very similar to that of the capillary, so the metastable effects may be exist in the short tube and this was confirmed by experiment [1]. Our previous studies of the capillary tube found that the Chen's metastable model is not ideal for R22, but reasonable results were obtained for R134a. The present short tube model will use Chen's metastable correction to verify the experimental short tube data for R134a.

PROPOSED MODEL

The present model is based on the governing Equations of Equation 1,5, and 10. The friction factor is calculated from Equation 15, in which Re is defined by Equation 16. For two-phase viscosity, Dukler mixing rule is selected. The metastable model proposed by Chen et al is also included in the present model.

Usually, two calculating methods can be used to calculate the mass flow rate of a tube when the dimension and the inlet and outlet conditions are known, one is from the inlet of the capillary tube marching step by step downstream to the exit [10], the other is from the exit back to the inlet step by step [25]. In the present model, the method from inlet to outlet is used.

The execution of the capillary tube flow model begins by defining

- the refrigerant,
- the tube geometry (Lc and dc),
- inlet and exit conditions (P_{inlet}, P_{outlet}, T_{inlet} or ΔT_{sc}),
- a constant incremental temperature drop for the two-phase region, and
- an initial assumed value for the mass flow rate.

Due to the more complicated flowing phenomena of short tube, the model was divided into two parts, one is the quality inlet case, the other is the subcooled inlet case.

Two-phase inlet case (quality inlet)

The model's general solution scheme involves the variation of the mass flow rate variable until the calculated tube length agrees with the actual length and all the constraints on the final flow solution are satisfied.

Given an initial mass flow rate value, the inlet pressure drop due to fluid acceleration and sudden contraction can be calculated from Equation 22 by knowing the entrance loss factor K, the upstream pressure (or temperature), the upstream quality (so the volume in Equation 22 can be calculated) and the short tube diameter (Gc=mass flow rate/cross section area of the short tube). By knowing this pressure drop, the inlet pressure of short tube can be calculated by subtracting this pressure drop from the upstream pressure, and the inlet quality can be calculated by assuming that this pressure

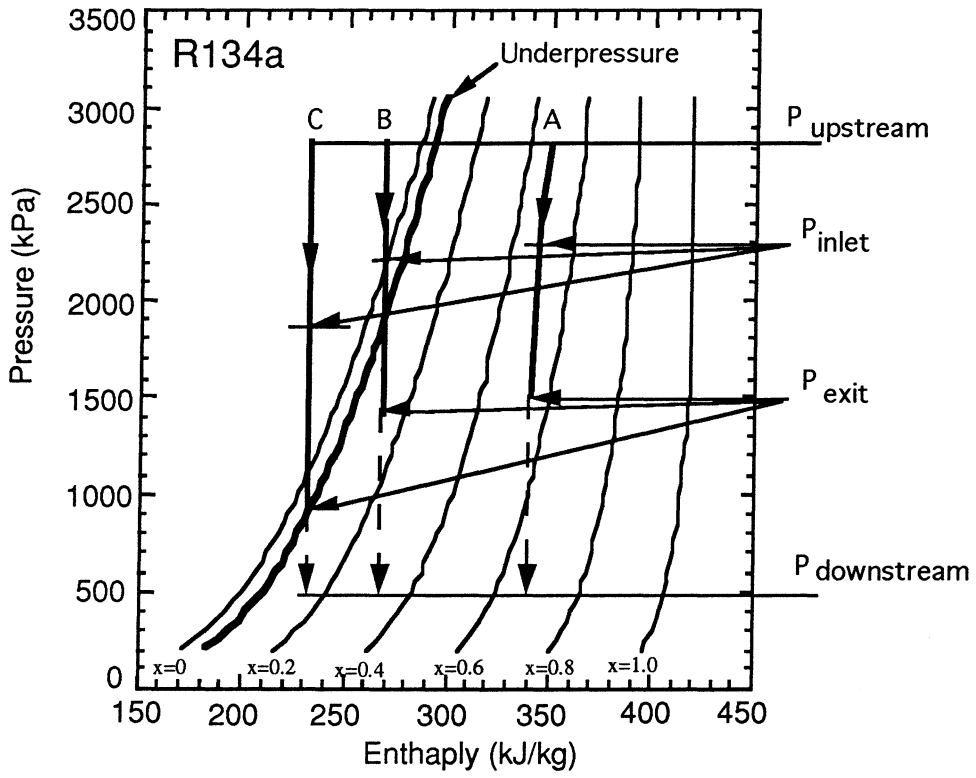

Figure 4 Schematic diagram of the process on P-h diagram

drop is isenthalpic, as shown in Figure 4 (for case A). After obtaining the pressure at the inlet plane, the equations are integrated step by step by selecting a constant pressure step and marching the total length of the tube, and checking the exit pressure. If the exit pressure is higher than the downstream pressure, the critical mass flux is evaluated using Equation 33. If the calculated critical exit pressure is less than the downstream pressure, a nonchoked flow condition exists, so

we have subcritical flow with the exit pressure equal to the downstream pressure and the flow solution is complete. The second law of thermodynamics is applied at each step in this process to ensure that ds>=0 for each segment. The choked mass flow rate is indicated by ds=0.

Single phase inlet case (subcooled inlet)

The subcooled inlet case is more difficult than the quality inlet case. Until now, there has been no theoretical model published for this case; most of the models are correlations from the experimental data based on the general orifice equation.

The mass flow rate of the short tube depends on the inlet condition (pressure and subcooling), tube dimension (diameter and length) and exit condition (usually exit pressure). For a given tube, the flow in the tube can be divided into three categories due to different upstream and downstream conditions: (1) the flow may be totally liquid (case C in Figure 4); (2) initially liquid flow and then flashed to two-phase flow and choked in the exit of the tube (like that in the capillary tube case, case B in Figure 4) and (3) after the contraction pressure drop, the inlet plane pressure is lower than the saturated pressure corresponding to the given subcooling, and the flow in the tube is totally two-phase (a special case of B).

For case B, as shown in Figures 4 and 5, the present capillary tube model can be used directly. The liquid length is calculated directly using Equation 6, which is rewritten below in terms of the known parameters:

$$\Delta L_{liq} = \frac{2\Delta P_{liq} d_c}{fvG^2} \tag{33}$$

The ΔP_{liq} term in Equation 33 is the difference between the liquid pressure just inside the short tube (after accounting for the inlet pressure drop) and the pressure corresponding to the onset of vaporization. When ΔP_{liq} includes the under pressure level calculated using the Chen's model, the liquid length, ΔL_{liq}, sets the flashpoint location inside the tube.

Starting at the flashpoint and throughout the two-phase region, the model assumes the existence of the thermodynamic equilibrium. The solution scheme "marches" downstream from the flashpoint across incremental lengths (Figure 1). For each segment, the entering flow condition is known; the exit temperature is defined by the specified pressure increments.

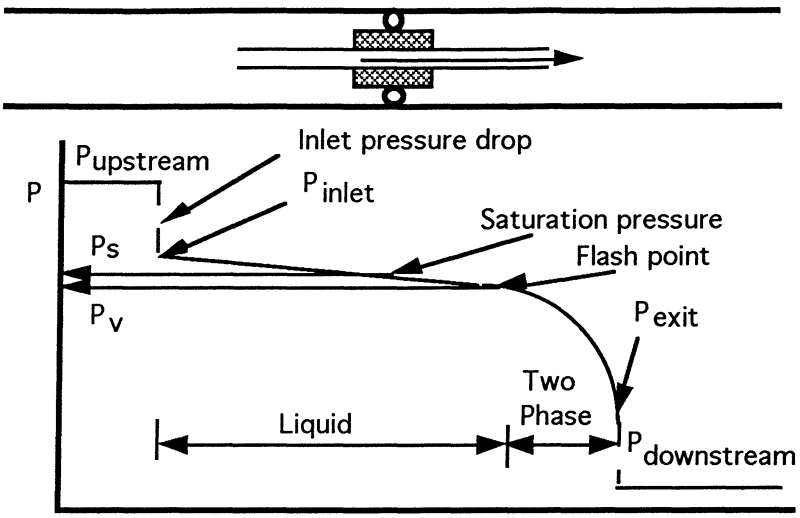

Figure 5 Short tube with subcooled inlet and two-phase exit

In determining the complete set of flow conditions at the exit of an incremental length, the continuity equation (Equation 1) is first combined with the energy equation (Equation 11) and yields a quadratic equation in terms of the exit quality x2 of the incremental length. Using the quality, the thermodynamic properties, velocity, and the friction factor at the exit of the axial incremental section can be determined, and then, the unknown incremental length, ΔL, can be calculated using the two-phase momentum equation (Equation 7). The flow solution proceeds downstream until the accumulated tube length is equal to the actual total length.

A constraint on the flow solution is provided by the second law of thermodynamics. In the case of adiabatic flow, this means that the entropy change in the direction of the flow can never decrease. As the calculated solution proceeds down the capillary tube, the entropy change across each incremental length is checked to ensure that the change is positive. If a second-law violation occurs, the mass flow rate variable is adjusted (decreased) and the solution procedure is restarted at the entrance to the tube [10].

The calculation for the slightly subcooled case C is straightforward, except for the iterations to locate the flash point, otherwise it is similar to case A, because the two-phase exit is choked. The situation for the highly subcooled case C is rather complicated. A new physical model is needed because experimental results suggest that the flow is choked because mass flow is independent of downstream pressure. However the presently available model, with or without metastable correction, predicts that the fluid at the exit of the tube is subcooled liquid.

Because of the length of the short tube orifice is shorter than the capillary tube, if the inlet subcooling is high enough, the fluid in tube should remain in liquid phase due to the small friction effect in the short tube. For this case, if we know the exit pressure of the short tube, the mass

flow rate can be calculated from Equation 32 (this is the application of momentum equation) directly:

$$G^2 = 2\frac{\Delta P d_c}{Lfv} \tag{32}$$

For doing this calculation, the exit plane pressure is needed, but practically, we only know the downstream pressure in the evaporator.

Model for highly subcooled inlet case

Figure 6 shows the experimentally measured mass flux for subcooled inlet case. Hrnjak [26] measured mass flow rate for 5 tube diameters, with and without upstream and downstream screens, over a wide range of two-phase and subcooled inlet conditions. If we suppose

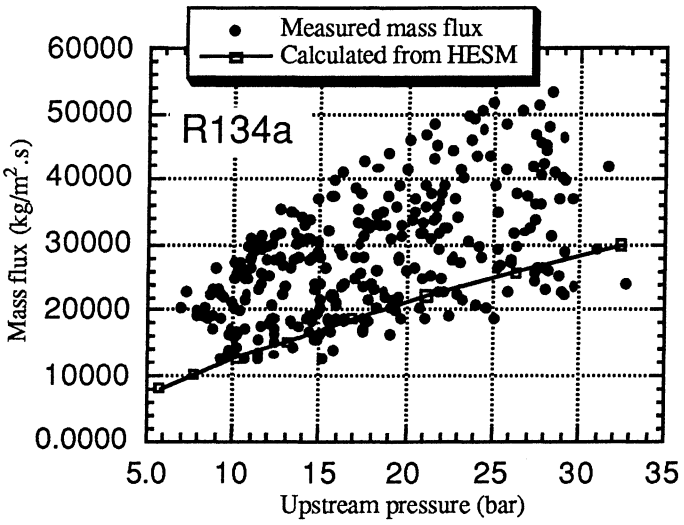

Figure 6 Measured mass flux and the calculated critical mass flux

all the flows are choked in the two-phase region, the critical mass flux can be calculated from Equation 28 by knowing the saturated pressure (or temperature) and quality. From Figure 3, it can be seen that the mass flux for a given saturation pressure is highest at low quality and at high saturation pressure. Therefore, the maximum upper bound on critical mass flux for a subcooled inlet data can be calculated by assuming zero pressure drop (saturated at the upstream pressure) and very low exit quality. The line in Figure 6 show this calculated upper bound. It is clear that, for subcooled inlet data, most of the data points lie above the line and are therefore not consistent with the assumption that the flow is choked in the two-phase region.

For a data point with high subcooling, after the inlet pressure drop due to sudden contraction and acceleration, the pressure at the exit plane may be still higher than the corresponding saturation pressure. The liquid can not be choked inside the tube because its velocity is far below the speed of sound in liquid. Therefore the pressure gradient tends to increase the mass flow rate, which in

turn increases the pressure and the frictional pressure drop in the tube. The exit pressure, decreases to the downstream pressure, allowing the mass flow rate to be calculated from Equation 32 directly. But for most of the cases, the downstream pressure was much lower than the exit pressure, and also lower than the corresponding saturation pressure. Therefore, the exit pressure will decrease to a point slightly less than the saturation pressure due to the metastable effect as shown in Figure 4. Therefore, the lowest possible exit pressure for

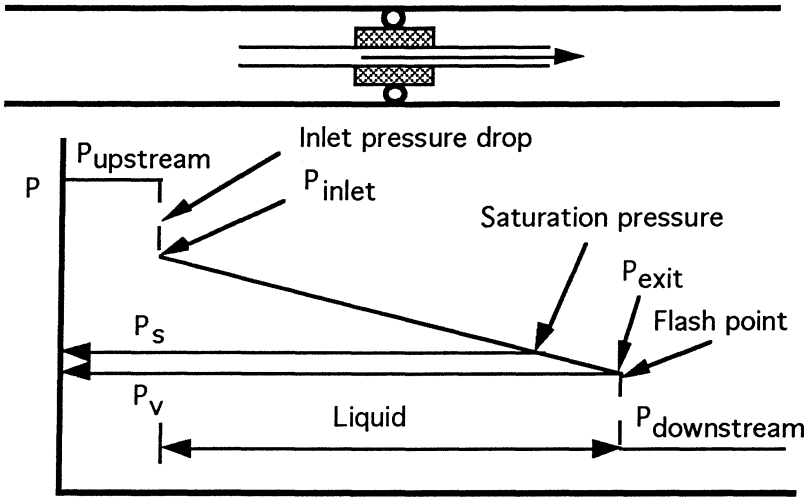

Figure 7 Physical model for subcooled exit data

this case is the saturation pressure as shown in Figure 7 (the metastable effect is also included), where the fluid at the exit plane is in the liquid state with zero quality. Because of the discontinuity in sound velocity between the liquid and two-phase regions, it is difficult to calculate critical mass flux for this case. But we know from the preceeding analysis that the exit pressure is very close to the saturated pressure, and the flow inside the tube must be subsonic liquid flow. Therefore the flash point must occur just outside of the exit section of the tube, followed by rapid expansion and two-phase choking at a cross-sectional area larger than the tube area, accounting for the high mass fluxes observed experimentally and shown in Fig 6. The mass flow rate at the exit plane can be calculated from Equation 32 directly using the total liquid-region pressure drop of

$$\Delta P = P_{inlet} - P_{exit}$$

$$= P_{inlet} - P_v \qquad (34)$$

where Pv is the pressure of vaporization after accounting the under pressure from Chen's metastable model: $P_v = P_{sat} - \Delta P_{sv}$. The metastable correction has a positive effect for mass flow rate.

COMPARISONS WITH EXPERIMENTAL DATA

The entrance pressure drop factor K is a very important factor for the subcooled inlet data. Idelchek's correlation suggests that a value of 0.5 should be used for this calculation, but our experiments showed that systematic mass flow rate deviations are exist when this K was used. As pointed out by Collier and Thome, none of the empirical methods for pressure drop prediction is suitable for every case. Since most correlations for entrance loss are based on experiments with water or steam-water mixtures, it may not applicable to this case, so the K value was determined from the quality inlet data as shown in Figure 8, by minimizing the mean squared error in mass flow rate. Only the quality inlet data were used for this estimation, to eliminate metastable effects. A value of 0.17 was obtained for the case of tubes having screens.

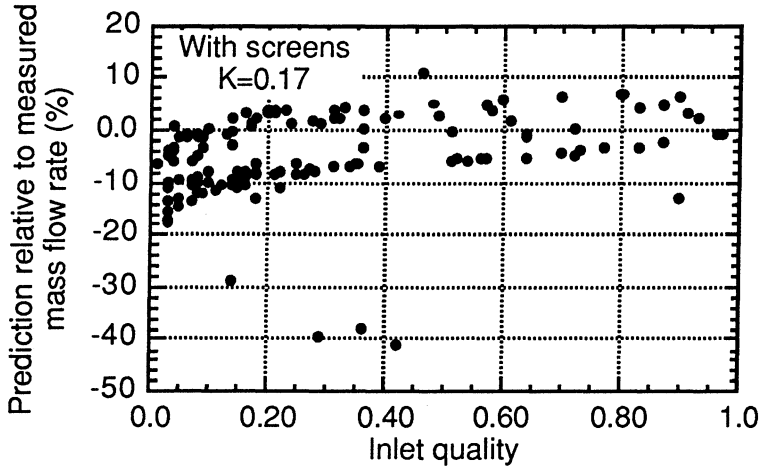

Figure 8 The prediction relative to measured mass flow rate.

As shown in Figure 8, the model tends to under predict the mass flow rate at low inlet quality. This is consistent with upstream sight glass observation of stratified flow, and the fact that inlet quality is calculated from measured heat addition to upstream subcooled liquid flow. For low quality cases, there are only a few bubbles produced, and these small bubbles may rise to the upper portion of the tube, above the orifice inlet. The under production may simply reflect the partial loss of small amounts of heat addition, and the presence of more saturated liquid entering the short tube orifice. For low quality region, there was more scatter in the data than in the high quality region, so the K value was determined from the data having $x>0.3$.

Figure 9 shows the comparison of predicted and measured mass flow rates, for all data points with inlet and outlet screens. It demonstrates that the proposed model can predict most of the experimental data points within ±10% for tubes with screens. The same inlet contraction loss

coefficient, K=0.17, was used for all cases. The experimental data covers the parameter ranges, with subcooling from 0°C to 50 °C, and inlet pressures as high as 35bar, and inlet quality from 0 to 0.98.

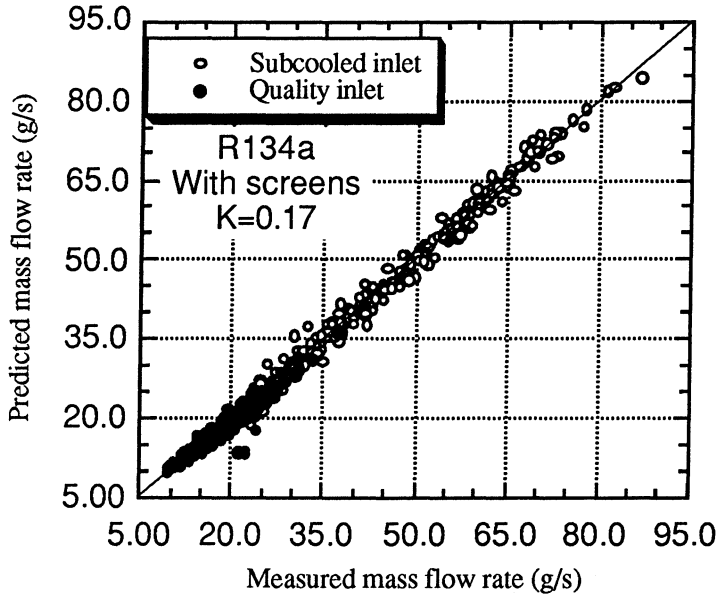

Figure 9 Model predictions compared to measured data

Figure 10 shows the mass flow rate predictions relative to the measured data for the tubes with screens. The results show systematic deviations for tubes having different inner diameters, for both quality inlet data and subcooled inlet data. The original experimental test was based on six different tubes with two tubes having same nominal diameter (inner diameter is 1.32 mm, as shown in Figure 10). For tubes with inner diameter of 1.45 mm and 1.70 mm, the average deviation between measured and predicted mass flow rate is close to zero, but for the tube with inner diameter of 1.55 mm, about -5% systematic deviations are observed. Similarly for the tube with inner diameter of 1.22 mm, a 4% systematic deviation was observed. For one of the tubes with inner diameter of 1.32 mm (Gray #13) about a -8% systematic deviation exists between predicted and measured mass flow rate. This may be caused by the tube roughness or uncertainties of tube inner diameter, because nominal diameters were used in the calculation. Further study of the tube roughness and inner diameter are needed in order to improve the accuracy of the model prediction. For a second 1.32 mm tube (Gray #14) there was only subcooled data, and the mean deviation was about 0.2% (data not included in Figure 10).

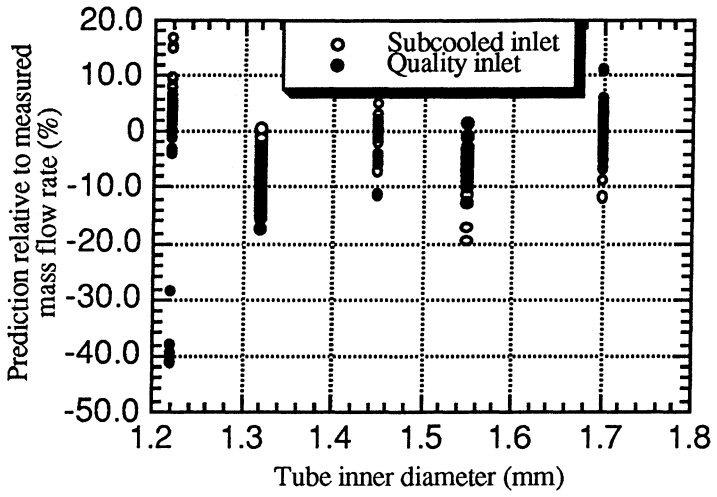

Figure 10 Flow rate predictions relative to the measured data

For the data without inlet and outlet screens, the model predictions exhibit large scatter exists for tubes having different lengths, making the determination of the K factor more difficult than the case for with screen data. Because these different lengths were obtained by cutting at the exit from the standard length (38.4 mm), the deviations of data for different length may have been caused by the effect of the cuts on the exit area. In order to determine the K factor for no-screen data, the quality inlet data with standard length was used, to eliminate possible biases due to tube cuts and metastable effects. A value of about 0.25 was found. Applying this K to subcooled inlet data, similar results were obtained.

Figure 11 shows the model prediction relative to measured data for no-screen tube for quality and subcooled data. Some systematic deviations exist for tubes of different lengths. However the model appears to predict quality inlet and subcooled inlet data with similar accuracy.

Figure 12 compares the model prediction with the measured data. As shown in this Figure, there is large scatter for some data, the reasons for this are not clear.

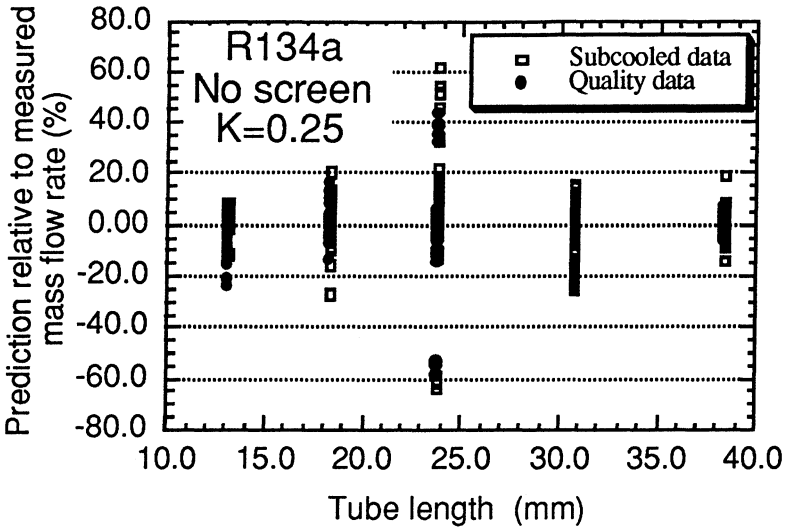

Figure 11 Flow rate prediction relative to the measured data

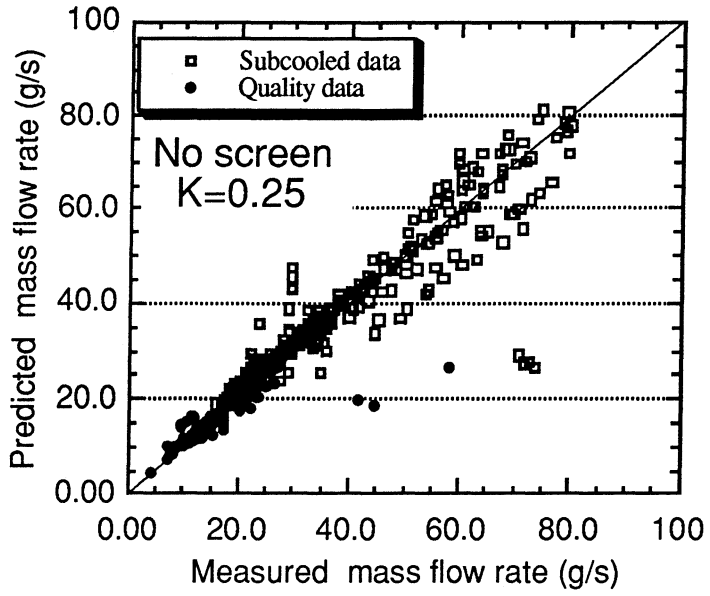

Figure 12 Model predictions compared to measured data

MEASUREMENT OF THE TUBE INNER DIAMETER AND ITS EFFECT TO MASS FLOW RATE

As shown in Figure 10 for quality and subcooled inlet data, there are some systematic deviations between the predicted and measured mass flow rate for tubes with different inner diameters. This may have been caused by tubes having different roughness, different inlet shape or the uncertainties of the tube inner diameter. In order to verify the tube inner diameter, experimental test were carried out for tubes with different inner diameter. Firstly, the tube was

carefully cut at the exit section close to the middle plastic seal gasket using a diamond cutter, and then the cross-sectional surface was carefully polished. Then it was measured under a microscope with 200X magnification. Diameter was measured in two orthogonal directions as shown in Figure 13. Table 2 show the experimental results.

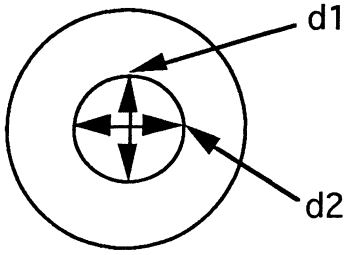

Figure 13 Short tube diameters

Table 2 Measured results for tube inner diameters

Tube color, number/nominal diameter (mm)	Measured diameter from two directions d1/d2	Area deviation between measured and nominal (%)	Mass flow rate factor due to area deviation (%)
Brown #07 /1.22	1.210/1.200	-3.36	-2.2~-4.8
Green #05 /1.32	1.340/1.345	2.96	no data
Orange #06 /1.45	1.455/1.450	0	0
Red #09 /1.55	1.585/1.580	3.76	2.8~3.8
Blue #15 /1.70	1.710/1.700	0.59	~1
Gray #19 /1.32	1.350/1.355	5.4	~6

The new diameters were then used to recalculate the mass flow rate, as shown in Table 2. The effect of area on mass flow rate, according to the model, depends on inlet conditions, and the effect might be magnified slightly for tubes with smaller diameter. All the area corrections reduce the deviations that were shown in Figure 10, so using the microscope or other methods to measure the "actual" inner diameter is a very important work for modeling the mass flow rate of short tube or capillary tubes.

Because the tubes had to be cut to fit under the microscope the dimensions shown in Table 2 are not the same tubes in which for measure the R134a mass flow rate was measured. They did, however, perform identically to the tested tubes in the nitrogen gas calibration test results (Hrnjak [26]). One exception was the set of Gray (nominally 1.32 mm) tubes, which exhibited substantial scatter on the nitrogen tests. Three more of these tubes were cut, and the diameters were measured (1.342/1.345, 1.335/1.332, 1.345/1.350 mm). The scatter in the nitrogen calibration tests is consistent with these relative diameters. Because of the scatter exhibited by the gray tubes' nitrogen flow data, none of them were tesd with R-134a; the 1.32 mm tube results shown in Figure 10 are all for the green tubes. For all the tubes tested, however, the observed difference

between normal and measured diameters would be large enough to account for the bias shown in the data of Figure 10.

Therefore the results here can, to some degree, explain why systematic deviations exist for tubes with different nominal diameters. There may be some other reasons such as the tube roughness, thermophysical properties of refrigerant and the assumptions of the theoretical model.

CONCLUSIONS

A new mathematical model of refrigerant flow through short tubes was presented. The new model is essentially the same as the adiabatic capillary tube model for quality inlet and low subcooling inlet cases. For high subcooling case, on the other hand, additional assumptions regarding the fluid state at the tube exit were proposed. When the model is applied to tubes with screens, the model can predict most of the experimental data for R134a within ±10%. If we use the measured inner diameter instead of the nominal diameter, the deviations can be reduced further. For no-screen case, the model based on nominal diameter predicted most of the experimental data with ±20%. The new model can be used over wide parameter ranges, with subcooling from 0°C to 50 °C, and inlet pressures as high as 35bar, and inlet quality from 0 to 0.98.

By analyzing Hrnjak's data with the theoretical model, it was found that the mass flow rate is very sensitive to the inlet pressure drop factor K for the subcooled inlet case. The published K correlations appear to be unsuitable for this case, the K value was determined from quality inlet data where no metastable effects were present. There is only a small difference between the K values for tubes with and without screen.

Model prediction results show that for tubes that have been cut to different lengths, there are some systematic biases at some lengths. This could have been caused by the cut affecting the diameter, but the reasons are still unclear. Overall the confidence in the entrance loss coefficient was reaffirmed by these tests.

The tube inner diameter needs to be measured to determine an "actual" diameter other than nominal diameter. The existence of some diameter-related deviations between measured data and model predictions result make it difficult to distinguish between metastable effects and tube roughness. Realistic values of tube roughness would have a small but negative effect on the mass flow rate, while metastable liquid flow has positive effect.

The metastable correction proved very important for adiabatic capillary tube modeling, and was also found here to be important for short tube modeling. Unfortunately the only published metastable model is restricted to limited parameter range and only for R12. Further experimental tests, especially for different refrigerants and for different tube dimensions, are needed in order to improve on Chen's published metastable model.

NOMENCLATURE

A	= flow area, m^2
c	= sonic velocity, m/s
d	= tube inner diameter, mm
D_c	= short tube nominal inner diameter, mm
D'	= reference length, m
e	= tube inner surface roughness, mm
f	= friction factor
G	= mass flux, $kg/s.m^2$
G_c	= critical mass flux, $kg/s.m^2$
h	= enthalpy, kJ/kg
k	= Boltzmann constant, J/K
K	= entrance pressure drop factor
L	= short tube length, mm
ΔL	= incremental length, mm
$\dot{m}$	= mass flow rate, g/s
P	= pressure, Kpa
$P_{downstream}$	= downstream pressure (evaporator pressure), Kpa
P_{exit}	= short tube exit plane pressure, Kpa
P_{inlet}	= short tube inlet plane pressure, Kpa
$P_{upstream}$	= upstream pressure (condenser pressure), Kpa
P_s	= saturation pressure, Kpa
P_v	= vaporization (metastable) pressure, Kpa
ΔP	= pressure difference, Kpa
Re	= Reynolds number
T_{crit}	= critical temperature, K
Ts	= liquid temperature, K
ΔT_{sc}	= inlet subcooling, K
V	= velocity, m/s
v	= specific volume, m^3/kg
x	= quality

Greek Symbols

ρ	= density, kg/m^3
σ	= liquid surface tension, N/m
μ	= viscosity, kg/s.m

Subscripts

f	= saturated liquid property
g	= saturated vapor property
liq	= liquid
m	= average property value over the incremental length
s	= constant entropy

REFERENCES

[1] Pasqua, P.E., 1953, "Metastable flow of Freon-12," *Refri. Eng.*, Vol. 61, pp. 1084-1088.

[2] Baily, J.F., 1951, "Mestable flow of saturated water," *Trans. of ASME*, Vol. 73, pp.1109-1116.

[3] Fauske, H.K., 1965, "The Discharge of Saturated Water Through Tubes, *Chemical Engineering Symposium*, Vol.61.

[4] Henry, R.E., 1970, "The Two-Phase Critical Discharge of Initially Saturated or Subcooled Liquid" *Nuclear Sci. Eng.*, Vol.41, No.3, pp.336-343.

[5] Aaron, A.A. and P.A. Domanski, 1990, "Experimentation, Analysis, and Correlation of Refrigerant-22 Flow Through Short Tube Restrictors," *ASHRAE Transactions*, Vol.96(1), pp. 729-742.

[6] Kim, Y. and D.L. O'Neal, 1993, "An Experimental Study of Two-Phase Flow of HFC-134a Through Short Tube Orificed, Heat Pump and Refrigeration Systems Design, Analysis, and Applications, *ASME winter meeting*, AES-Vol. 29, pp1-8.

[7] Kim, Y. and D.L. O'neal, 1994, "Two-Phase Flow of R-22 Through Short Tube Orifices," *ASHRAE Transactions*, Vol. 100(1).

[8] Moody, F.J., 1965, "Maximum Flow Rate of a Single Component Two-Phase Mixture," *Journal of Heat Transfer, Trans. ASME series C*, Vol. 87, No.1, pp.134-142.

[9] Levy, S., 1965, "Prediction of Two-Phase Critical Flow Rate," *Journal of Heat Transfer, Trans. ASME series C*, Vol. 87, No. 1, pp. 53-58.

[10] Bittle, R.R., and M.B. Pate, 1991, "A Theoretical Model for Predicting Adiabatic Capillary Tube Performance with Alternative Refrigerants," *ASHRAE Transactions*, 97(1), pp. 1-12.

[11] Kuehl, S.J., and V.W. Goldschmidt, 1991, "Modeling of Steady Flows of R22 Through Capillary Tubes, *ASHRAE Transactions*, 97(1), pp. 139-148.

[12] Swamee, P.K., and A.K. Jain, 1976, "Explicit Equations for Pipe-Flow Problem," *Proceedings of the ASCE, Journal of the Hydraulics Division*, 102, HY5, pp. 657-664.

[13] McAdams, W.H., W.K. Wood, and R.L. Bryan, 1942, "Vaporization Inside Horizontal Tubes-II-Benzene-Oil Mixtures," *Transactions of ASME*, 64:193.

[14] Cicchitti, A., C. Lombardi, M. Silverstri, G. Soldaini, and R. Zavattarelli, 1960, Two-Phase Cooling Experiments-Pressure Drop, Heat Transfer, and Burnout Measurements," *Energia Nucleare,* 7(6), pp. 407-425.

[15] Dukler, A.E., M. Wicks, and R.G. Cleveland, 1964, "Frictional Pressure Drop in Two-Phase Flow-Part A and B," *AICHE Journal,* 10(1), pp. 38-51.

[16] Collier, J.G., and J.R. Thome, 1994, "Convective Boiling and Condensation," New York: Oxford University press.

[17] Idelchik, I.E., Handbook of Hydraulic Resistance, 1994 3rd Edition, CRC Press, Inc. p.197

[18] Melo, C., R.T.S. Ferreira, and R.H. Pereira, 1992, "Modeling Adiabatic Capillary Tube: A Critical Analysis," *1992 International Refrigeration Conference*, Purdue University, July 1992, pp. 113-123

[19] Hsu,Y. and R.W. Graham, 1976, "Transport Processes in Boiling and Two-Phase Systems," New York: Hemisphere Publishing Company.

[20] Smith, R.V., 1963, "Some Idealized Solutions for Choking, Two-Phase Flow of Hydrogen, Nitrogen and Oxygen," *Advances in Cryogenics Engineering*, Vol. 8, New York: Plenum, pp. 563-573.

[21] Wallis, G.B., 1969, "One-Dimensional Two-Phase Flow," New York: McGraw Hill Book Company.

[22] Pate, M.B., and D.R. Tree, 1987, "An Analysis of Choked Flow Conditions in a Capillary Tube-Suction Line Heat Exchanger," *ASHRAE Transactions*, Vol. 93(1).

[23] Chen, Z.H., R.Y. Li, S. Lin, and A.Y. Chen, 1990, "A Correlation for Metastable Flow of R-12 Through Capillary Tubes," *ASHRAE Transactions,* 96(1), pp. 550-554.

[24] Dirik, E., C. Inan, and M.Y. Tanes, 1994, "Numerical and Experimental Studies on Adiabatic and Nonadiabatic Capillary Tubes with HFC-134a," *International Refrigeration Conference Proceedings*, Purdue University, July, Vol. 1, pp.365-370.

[25] Mullen, C.E., B.D. Bridges, K.J. Porter, G.W. Hahn, and C.W. Bullard, 1997, "Development and Validation of a Room Air Conditioning Simulation Model," ACRC TR-116.

[26] Hrnjak, P.S., "Experimental Analysis of Orifice Tube Performance," ACRC TR forthcoming 1998.